

# Generating Tyre Geometries Incorporating Real Tyre Deformation for Aerodynamic CFD Analysis

Johannes Burgbacher, Leander Reichhart, Victor Mappes, Timo Kuthada, Felix  
Wittmeier, Andreas Wagner

Institute of Automotive Engineering (IFS)  
Pfaffenwaldring 12  
70569 Stuttgart  
johannes.burgbacher@ifs.uni-stuttgart.de  
leander.reichhart@fkfs.de  
victor.mappes@ifs.uni-stuttgart.de  
timo.kuthada@fkfs.de  
felix.wittmeier@fkfs.de  
andreas.wagner@ifs.uni-stuttgart.de

**Abstract:** For optimal flow predictions via computational fluid dynamics (CFD), a geometric representation that is as realistic as possible is necessary. Consequently, a process was developed as part of a research project, funded by the Forschungsvereinigung Automobiltechnik (FAT) with the aim to generate tyre geometries that accurately reflect real tyre deformation. The process involves a combination of structural light scanning and a newly designed and built tyre deformation test bench. Additionally, a parameter study was conducted on the tyre deformation test bench, to evaluate the influence of vertical tyre load, tyre pressure and rotational speed on the tyre deformation.

## 1 Motivation

Up to 25% of the vehicle aerodynamic drag is contributed by the wheels and the wheel arches [1]. This section of the car represents significant optimization potential for aerodynamic development. Aerodynamic optimizations mainly rely on wind tunnel testing and CFD. Wind tunnel testing is widely regarded as a highly accurate method for evaluating aerodynamic properties. However, during the initial stages of aerodynamic development, vehicle models are often unavailable. As a result, decisions regarding aerodynamic optimizations are primarily based on CFD simulations. Consequently, it is imperative that CFD models are highly accurate. The basis of all CFD applications is an accurate representation of the geometry being analysed. Supposedly, small geometrical changes of the tyre geometry have an influence on the flow around the tyre [2]. With respect to the geometric change due to tyre deformation, a multitude of studies with FEM generated tyre deformations have demonstrated the significant impact of tyre deformations on the wheel flow [3] [4].

When validating flow phenomena with FEM generated geometries, discrepancies between experimental and simulation results may arise due to errors in either the FEM or CFD. To address this issue, a process has been established to generate tyre geometries by combining a static, high-definition structural light tyre scan with the results from a new testing bench, that has been designed and built at the Institute for Automotive Engineering University of Stuttgart (IFS). This new tyre deformation testing bench enables to physically measure tyre deformations on rotating and loaded tyres, that can later be used for CFD studies.

This study is part of a research project funded by the Forschungsvereinigung Automobiltechnik (FAT) with the goal to investigate the effects of tyre deformation on vehicle aerodynamics and validate and improve CFD accuracy regarding this area.

## 2 Prerequisites

In automotive wind tunnel testing the road and the rotation of the wheels has to be represented accurately. This can be achieved using one or multiple belts to enable wheel rotation and simulate boundary layers on the ground. In typical 5-belt systems, the vehicle is constrained by rocker panel mounts. By restricting the body motion in some or all degrees of freedom, the vehicle can either be held in a fixed or a floating mounting configuration. In the floating configuration, only the longitudinal and lateral components of the forces are restricted. In the fixed configuration, the weight force from the vehicle is transferred both through the rocker panel mounts and the tyre. Additional aerodynamic loads from the vehicle body are mainly transferred through the rocker panels, while radial tyre expansion creates additional forces that impact the tyre position in the wheel house and the vertical load of the tyre. In the floating setup, vertical aerodynamic load results directly in vertical tyre load. Because the vehicle model is not vertically restricted in floating mode, additional forces from expanding rotating tyres result in a change in vehicle ride height and are therefore not additional vertical tyre loads.

## 3 Tyre Deformation Test Bench

Regardless of the vehicle mounting configuration during wind tunnel measurements, the overall tyre load condition on the tyre deformation test bench must match the overall tyre load condition from the wind tunnel measurement. To accurately represent the same tyre deformation in CFD as in wind tunnel testing and open road driving the tyre test bench must be a flat belt system. Additionally, the tyre pressure, track, camber, rotational speed, temperature, and tyre vertical load must be identical to generate the same tyre deformation in both the wind tunnel and the tyre test bench. Since measuring vertical tyre load in the wind tunnel is not easily accomplished, the vertical tyre load is represented as the static tyre radius  $r_{stat}$ , which represents the standing height of the tyre. It is measured or calculated as the z-normal distance between the wheel axis and the floor. Since measurement positions on the wheel axis with tyre camber can generate varying  $r_{stat}$  values, the measurement position is defined as the intersection of the wheel hub cover and the wheel axis.

Acquiring the geometry of a rotating tyre presents a significant challenge. The high rotational speeds and non-rotationally symmetric tyre geometries make mechanical scanning methods unsuitable. Optical measurement methods are possible, but the black, shiny surface of the tyre and its fast surface velocity present challenges for these methods as well. Preliminary investigations have shown that measurement methods such as high-speed photogrammetry are not cost- or time-effective. Structured light scanning methods were unable to accurately capture the rotating tyre geometry near the flat belt. The preliminary investigations indicated that laser line profile scanners are the most suitable optical measurement method in terms of accuracy and feasibility.

### 3.1 Tyre Deformation Test Bench Layout

The IFS Handling Roadway test bench (HRW) provides an ideal foundation for the tyre deformation test bench. In its original purpose, it is used for full vehicle dynamic research under laboratory conditions [5]. It consists of four independent flat belt units and a vehicle constraint, as shown in Figure 1. Each flat belt unit is capable of reaching speeds up to 220 km/h and can be hydraulically steered up to  $\pm 20^\circ$  and vertically actuated up to  $\pm 75$  mm. [5].

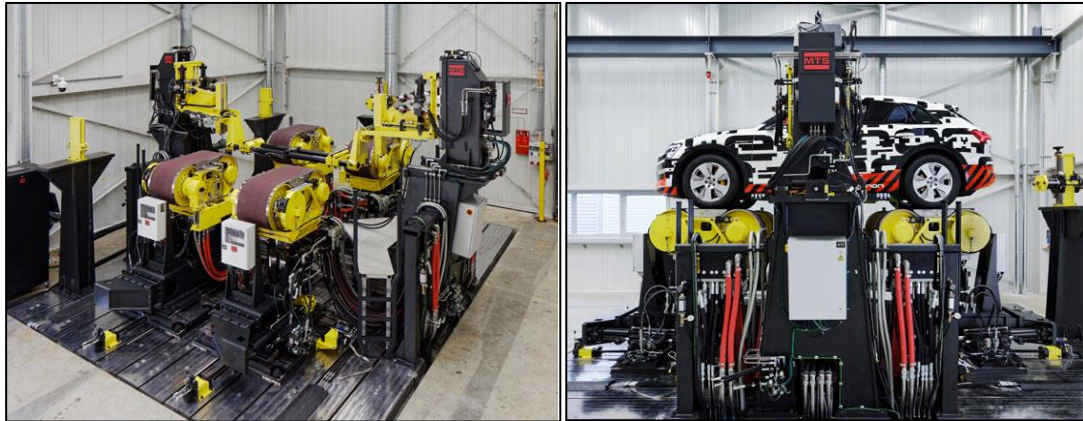


Figure 1: IFS Handling Roadway Test Bench [5]

To measure tyre deformations, the front left flat belt unit (relative to the vehicle) was augmented with a tyre measurement attachment, as shown in Figure 2. This attachment is mounted on two steel pillars. Prior to measurements, the flat belt is lowered to its minimum vertical position to facilitate tyre changes and accessibility.



Figure 2: Tyre Deformation Test Bench

During measurements, the wheel bearing remains fixed in position. A vertical tyre load is generated by hydraulically lifting the flat belt unit vertically, allowing for adjustment of the chosen static tyre radius  $r_{stat}$  as in wind tunnel measurements. The tyre velocity is provided by the movement of the flat belt unit. Five optical laser profile scanners are mounted on a pivot arm. During measurements, this pivot arm is rotated  $\pm 100^\circ$  from the vertical arm position around the wheel by a stepper motor combined with a worm drive. For each pivot arm position, 100 profiles are recorded and afterwards averaged to produce a point cloud representing the average deformation of the tyre.

Both the main frame and the camber frame are constructed from 10 mm thick welded steel profiles and are connected by two radial spherical plain bearings and two manually adjustable camber actuators, as shown in Figure 3. A vertical sledge with a linear bearing is installed to enable vertical load measurements. The wheel bearing is installed in distance to the camber frame, to provide the appropriate measurement distance for laser scanner sensors. The main frame, camber frame and vertical sledge need to withstand all forces acting on the tyre.

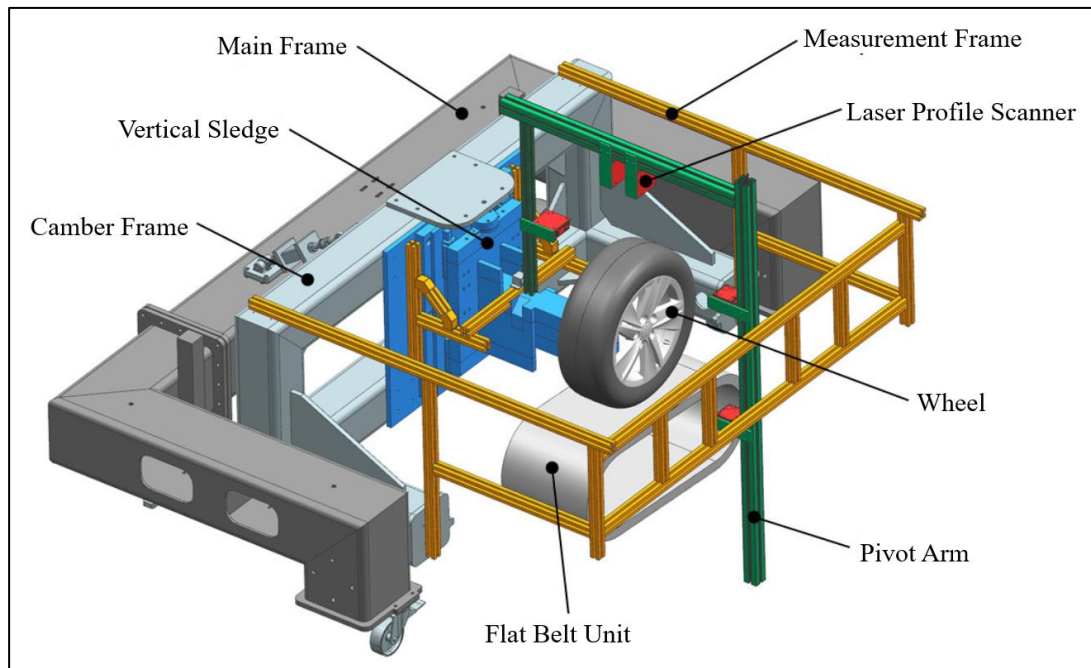


Figure 3: Tyre Deformation Attachment Layout

The measurement frame is positioned to align the wheel bearing and pivot arm bearing axis, as shown Figure 4. This layout satisfies the optimal laser scanner measurement distance for all pivot arm angle angles.

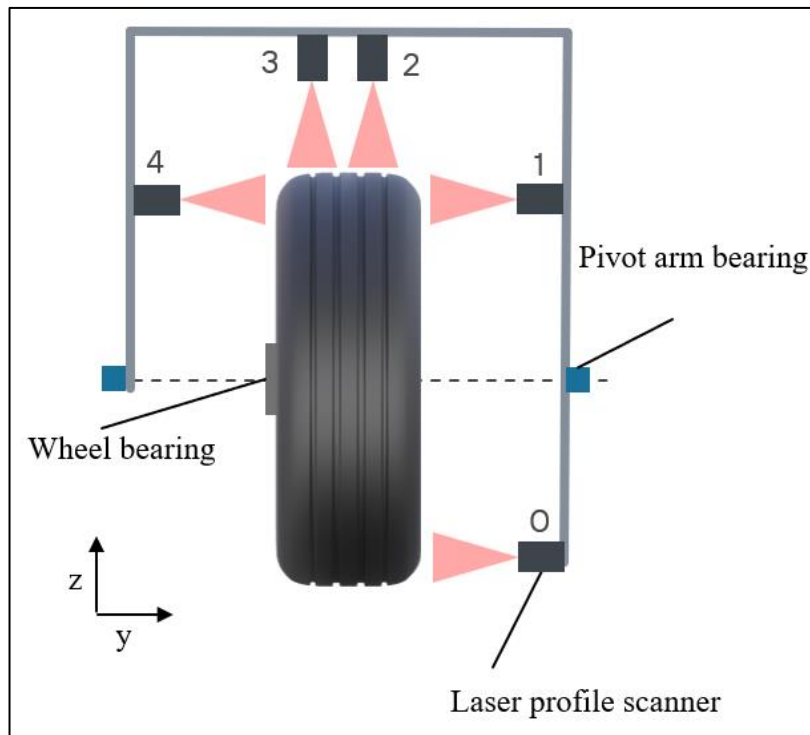


Figure 4: Sensor Layout

### 3.2 Tyre Deformation Test Bench Sensors and Data Acquisition

The software for recording measurements and controlling actuators has been implemented using LabVIEW code. Optical measurements are conducted via laser profile scanners, which operate on the principle of triangulation. Unlike distance sensors, which are equipped with a 1D line sensor to measure distances, laser profile scanners have a 2D sensor that can measure both height and distance coordinates [6]. The test bench is equipped with 5 laser scanners from micro epsilon. The sensors have a line linearity of 12  $\mu\text{m}$  and are connected to the measurement computer via Ethernet port.



Figure 5: Laser Scanner: micro epsilon scanCONTROL [8]

To rotate the sensors around the wheel, a stepper motor combined with a worm drive is installed, allowing the sensors to be positioned with an accuracy better than  $1^\circ$ . For scanning of a rotating tyre, a  $2^\circ$  step was chosen for giving good results in radial direction.

The HRW flat belt unit serves both as an actuator and sensor for speed, vertical tyre load and steering angle. It can be rotated hydraulically around its vertical axis to set tyre slip angles. The vertical tyre load is adjusted by vertical positioning of the flat belt unit using a hydraulic actuator.

A laser height sensor is mounted on the vertical sledge to measure the distance to the flat belt and is used to set up the flat belt vertical position in correspondence to the predefined  $r_{stat}$  values.

The vertical sledge and camber frame are connected by a load cell, allowing for the measurement of vertical tyre loads. A potentiometer is used to determine the absolute pivot arm angle and a tyre pressure monitoring system (TPMS) is used to track tyre air temperature and pressure.

### 3.3 Tyre Deformation Test Bench Measurement Procedure

Prior to a tyre deformation measurement the following parameters have to be defined:  $r_{stat}$ , the rotational speed and tyre pressure. Generally, adjusting one or more of these parameters results in a time relative temperature change of the tyre. This change in temperature impacts the tyre pressure. By keeping  $r_{stat}$  constant, this change in temperature results in a change in tyre vertical load and tyre deformation. Therefore, a state of equilibrium tyre temperature and pressure has to be set prior to each tyre deformation measurement.



During measurements, the tyre rotates at a constant speed and under constant vertical load. The following measurement process is automatized. First, a vertical load measurement is performed, then each pivot arm angle is traversed stepwise. At each pivot arm angle, measurements are performed for each laser profile scanner. In order to get a time averaged measurement result, each laser scanner records 100 samples for every measurement.

Two approaches of tyre deformation measurements are implemented: full measuring mode and single cut mode. In full measurement mode, the pivot arm is rotated in  $2^\circ$  steps  $\pm 100^\circ$  relative to the vertical position. On Figure 6 right, the measurement result of this mode is shown. This setup is used to measure tyre deformation for CFD studies.

In single cut capturing mode, only the vertical position of the pivot arm is measured, allowing for fast measurement of multiple tyre deformation parameters and tyre models and determining their deformation behaviour. Its result is shown on the left in Figure 6.

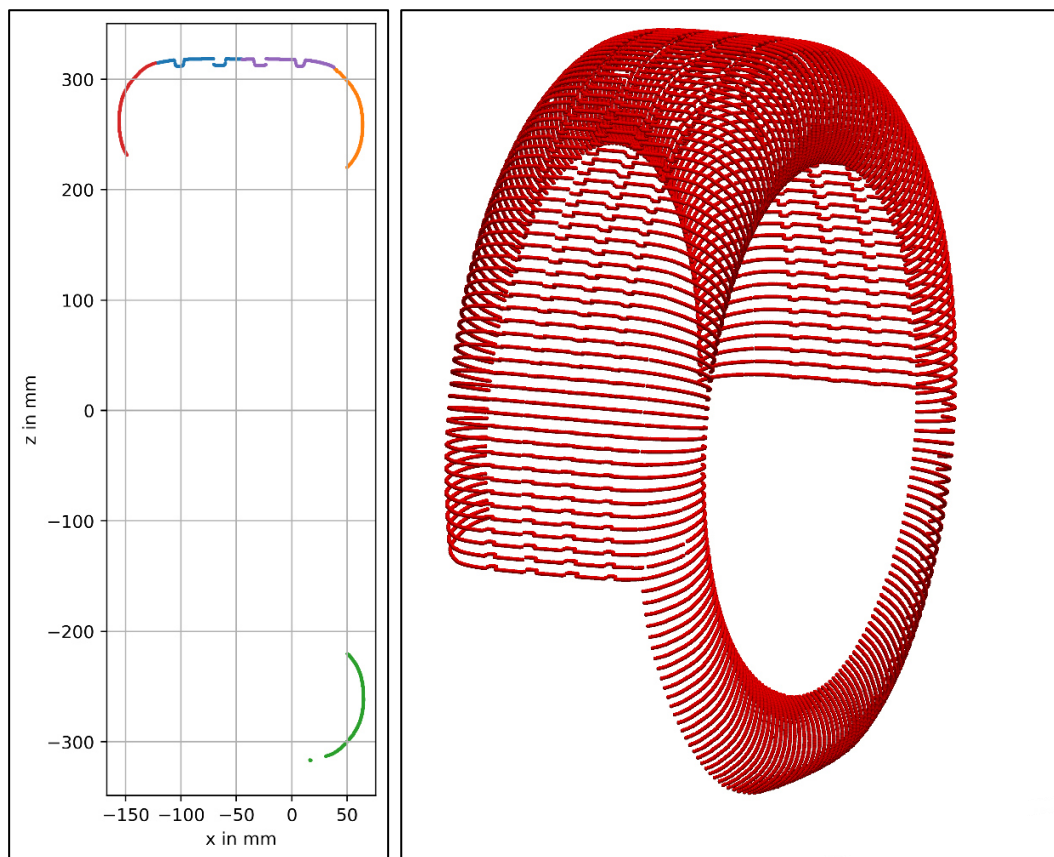


Figure 6: Left: Single Cut Deformation Capturing for rapid assessment of multiple parameters and tyres, with vertical pivot arm. Right: Full Deformation Measurement for the generation of CFD geometries with rotated pivot arm



### 3.4 Tyre Test Bench Post Processing

Post Processing is implemented using python code and is fed with the measurement raw data and a corresponding configuration file. The configuration file contains all additional data and instructions in order to average and coordinate transform the input data.

All sensor data must be coordinate transformed from the sensor coordinate system, to the wheel coordinate system using the sensor position on the pivot arm and the pivot arm angle. Then, the sensor data for each sensor is time averaged. Overlapping sensor areas must be automatically cut in a later step, and areas such as the floor and rims are deleted. The final result of the post processing routine can be seen in Figure 6 on the right and contains a point cloud of either a planar vertical section or a point cloud of the full tyre, depending on the measurement mode.

## 4 Process for Generating Tyre Geometries with Real Tyre Deformation

The process of generating tyre geometries with real tyre deformation involves combining a static tyre structural light scan with the results from the tyre deformation test bench measurement using a morphing function.

### 4.1 Static Structural Light Scanning

The structural light scan is performed on a static unloaded tyre and produces a high-resolution tessellated geometry representation of the tyre that captures fine details such as the tyre markings. Structural light scans rely on a projector and a camera positioned at a relative distance to each other, so they can only capture areas visible to both devices. Fine grooves or undercuts that cannot be captured result in holes, as illustrated by the white area in Figure 7 “Scan”. To overcome this issue, manual repairing, wrapping or reverse engineering the tyre as a cad model are options. The wrapped, reconstructed or a hybrid geometry and all defeatured versions thereof serve as a CFD geometries, as shown in Figure 7.

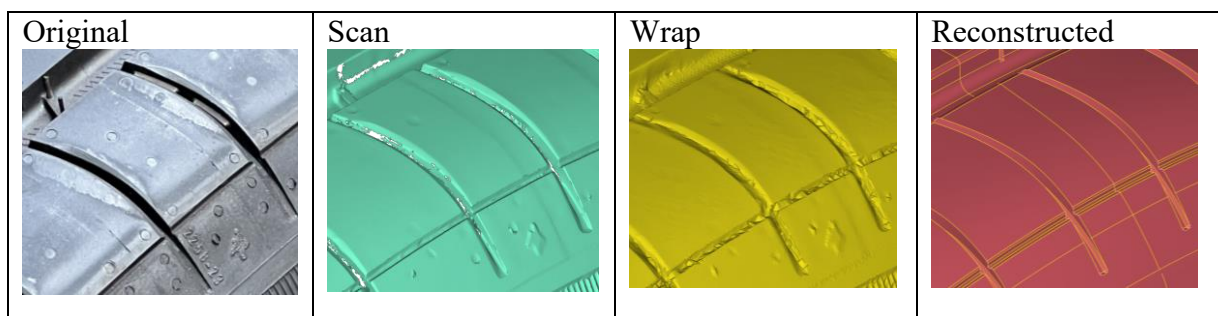


Figure 7: Static Tyre Scanning and CFD geometry generation

## 4.2 Morphing Process

The input to the morphing process is based on two inputs: The structural light scan or a defeatured version of it and a point cloud derived from the tyre deformation test bench measurement. The morphing process is implemented in ANSA. It is implemented in such a way that the same morphing function can be applied to multiple versions of the same tyre geometry regardless of its level of detail.

Prior to morphing, the input data must be pre-processed: based on the static tyre scan, a simplified slick tyre geometry is generated (as shown in Figure 8 a)) to serve as a construction basis for multiple Morphing Boxes. If not already tessellated, the undeformed tyre resulting from the tyre scan must be meshed and loaded into the morphing boxes. The point cloud derived from the deformation measurement is then reconstructed as a deformed slick tyre geometry using either manual CAD reconstruction or surface reconstruction.

By fitting the morphing boxes onto the deformed slick geometry, the loaded tyre geometry is deformed based on the deformation measurement. As a result, real deformed tyre scans or real deformed geometry derivatives of the tyre scans with a lower level of detail can be generated based on the real measured tyre deformation.

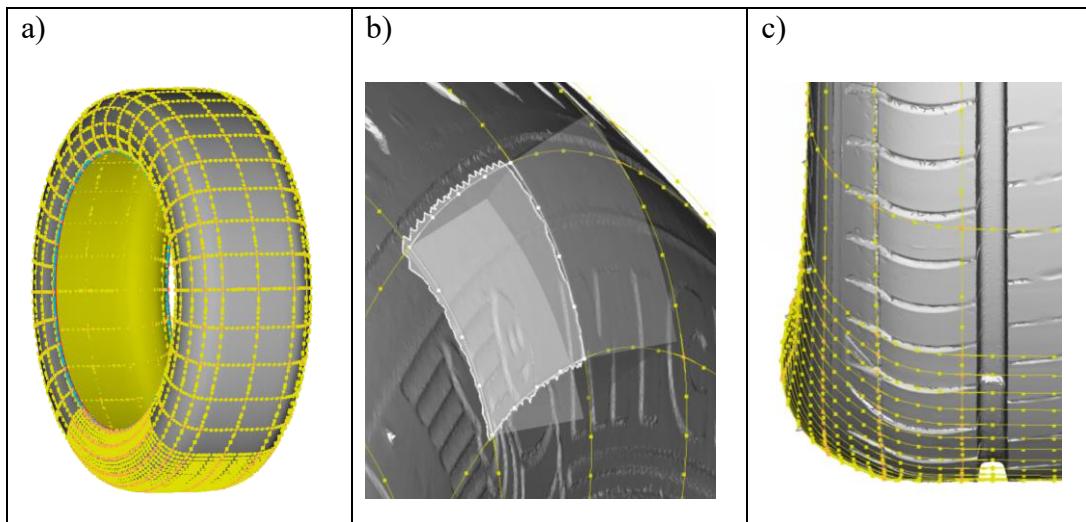


Figure 8: Tyre Morphing process. a) Fitting morphing boxes onto a slick tyre geometry b) Loading the tyre geometry into the morphing boxes c) Morphing the input tyre geometry by fitting the morphing boxes on the deformed slick tyre geometry deriving from the tyre deformation measurement

## 5 Results

A study was conducted to investigate the effects of tyre vertical load, rotational speed, and tyre pressure on tyre deformation using single cut measuring mode with the pivot arm in a vertical position. The tyre related parameters were selected based on a parallel wind tunnel campaign. The baseline configuration, from which each parameter was altered included an unloaded  $r_{stat}$  value at standstill, a tyre pressure of 2.5 bar, and a rotational speed of 140 km/h. Figure 9 illustrates the differences of the tyre deformation at three positions for five tyre models:

- $\Delta z$ : represents the difference in radial expansion at the top center position
- $\Delta y_{top}$ : represents the difference in axial expansion at the most outward y position at the top half
- $\Delta y_{bottom}$ : represents the difference in axial expansion at the most outward y position at the bottom

The Goodyear 19" tyre side wall shape features an exposed rim guard and  $\Delta y_{top}$  and  $\Delta y_{bottom}$  are calculated at this position.

The results indicate that an increase in rotational speed causes radial expansion and axial contraction of the tyres at both the bottom and top. Near to the flat belt, the tyre is unable to escape the flat belt. This inhibits axial contraction at the bottom compared to the top. In this study tyres with lower heights tend to exhibit lower axial contraction.

A decrease in tyre pressure results in radial contraction, with this effect being more pronounced for wider tyres. An increase in vertical load has the biggest impact on the change of shape, particularly on the tyre sidewall. Wider tyres have a larger contact area and can distribute the vertical load over a larger area, resulting in comparatively lower change in  $r_{stat}$  and lower axial expansion at the contact area for the same vertical load.

When comparing the 16" and 19" tyres with equivalent tyre dimensions, it is observed that the change in shape in response to a configuration change is dependent on the specific tyre model and cannot be generalized.

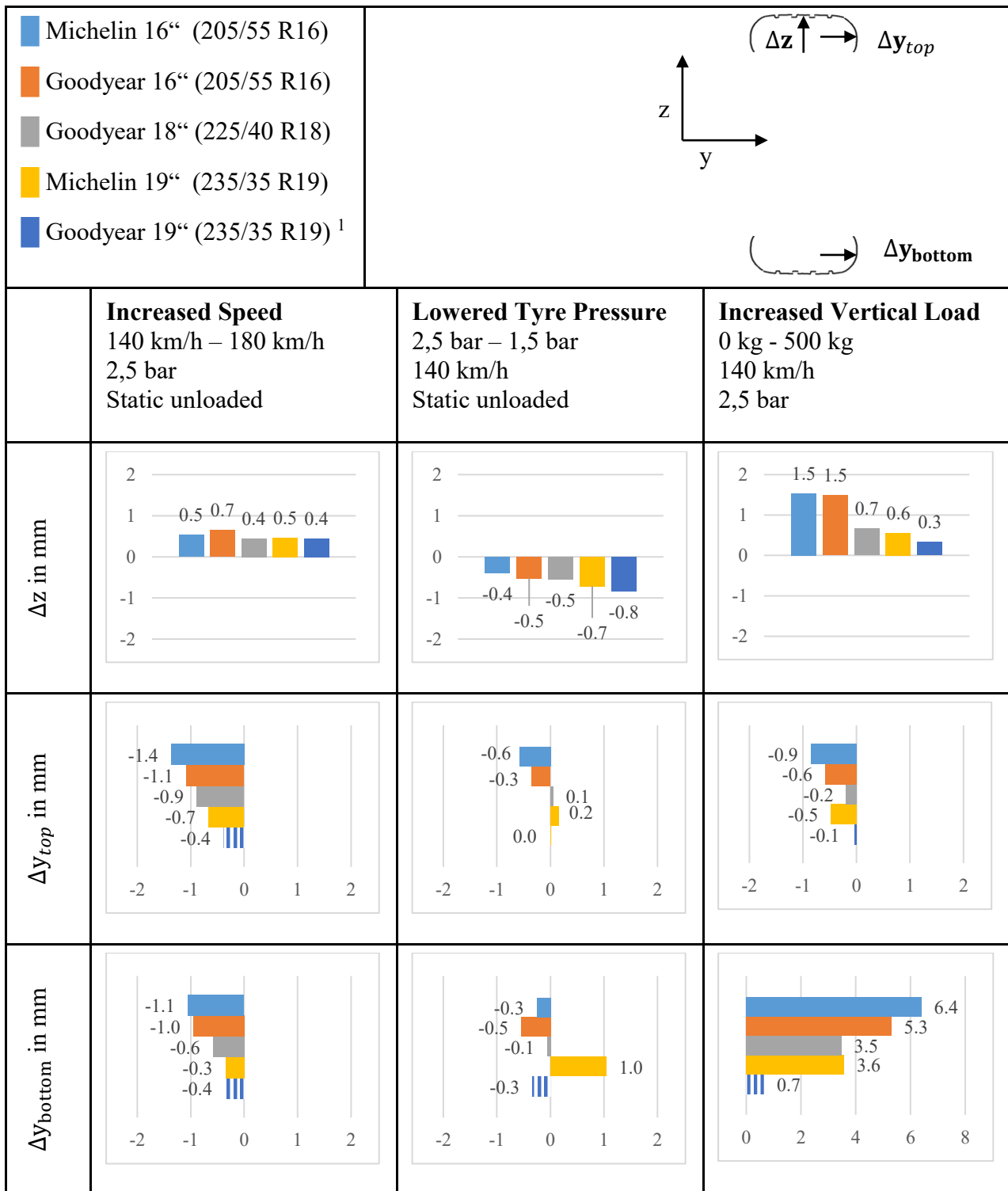


Figure 9: Parameter study results regarding tyre deformation parameters

<sup>1</sup> For the Goodyear 19" tyre, the widest position in y corresponds to the rim protection edge.

The combination of detailed, high-density structural light scanning and real tyre deformation provides an ideal basis for CFD studies. Figure 10 shows a comparison between experiment and geometry for a detailed tyre wrap. As previously mentioned, the process is not restricted to the wrapped tyre geometry and can be applied to all forms of tessellated tyre geometry.

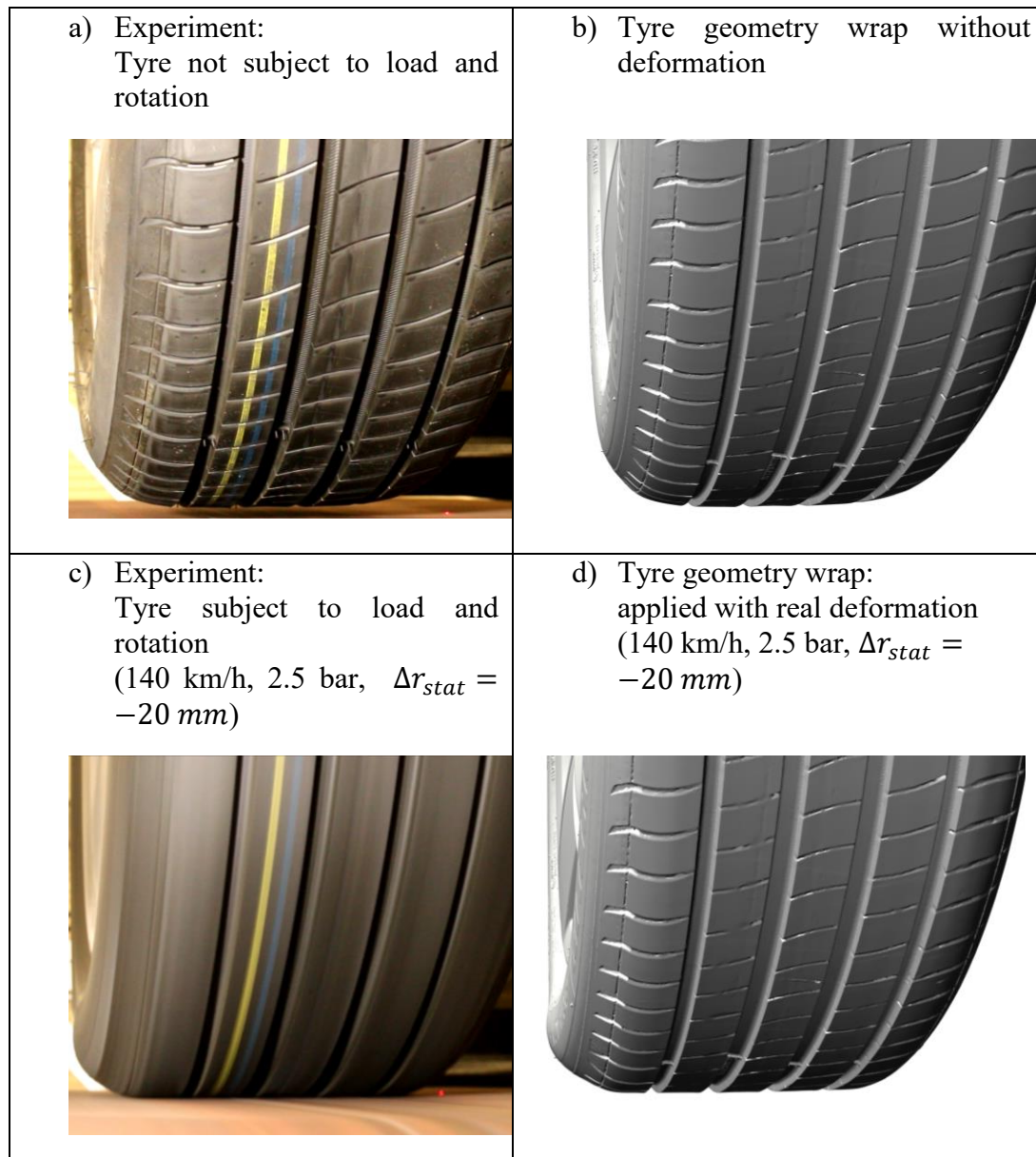


Figure 10: Undeformed tyre (top) and deformed tyre (bottom). Comparison between photographical image from the experiment (left) and geometry rendering (right)

## 6 Summary and Outlook

An accurate geometric representation is essential for all CFD studies, as even minor geometric changes to the tyre geometry can impact the aerodynamics of a vehicle. When driving a vehicle on the road, tyres are subject to rotation and load, resulting in changes to their shape compared to an undeformed, stationary tyre. To improve future CFD flow prediction for vehicle aerodynamics, a process has been established to generate high-quality tyre geometries that accurately reflect tyre deformation.

A tyre deformation test bench has been built, to reproduce and measure tyre deformation under conditions similar to those encountered during open road driving and wind tunnel measurements. A morphing process has been established, to combine structural light scans and tyre deformation measurements. Additionally, a parameter study was conducted to investigate the effects of vertical tyre load, tyre pressure and rotational speed on tyre deformation. Changes in tyre pressure have comparably lower effects on overall tyre shape, while rotational speed and vertical tyre load have a larger impact on the tyre deformation. The tyre deformation is dependent on both the tyre type and dimensions of the tyre.

The geometries generated using this process serve as the basis for future CFD studies. As part of this research project an extensive wind tunnel measurement campaign at the IFS Vehicle Aeroacoustics Wind Tunnel was already conducted using a DrivAer Model from Volkswagen to serve as a validation basis for this CFD study.

## 7 Bibliography

- [1] Pfadenhauer, M.; Wickern, G.; Zwicker, K.: On the Influence of Wheels and Tyres on the Aerodynamic Drag of Vehicles. MIRA International Conference on Vehicle Aerodynamics, Birmingham, 1996
- [2] Wittmeier, F.: Ein Beitrag zur aerodynamischen Optimierung von Pkw Reifen, Springer Vieweg Wiesbaden , 2014, <https://doi.org/10.1007/978-3-658-08807-1>
- [3] Eder P.; Gerstorfer, T.; Lex, C.; Amhofer, T.: Tyre Deformation Modelling for High-Speed Open-Wheel Aerodynamic Investigations. In: SAE International Journal of Vehicle Dynamics Stability and NVH, 5 (2021), no. 3, article 10-05-03-0016
- [4] Semeraro, F.F.; Schito, P.: Numerical Investigation of the Influence of Tyre Deformation and Vehicle Ride Height on the Aerodynamics of Passenger Cars. Online: <https://www.mdpi.com/2311-5521/7/2/47#>, accessed: 17. August 2023

- [5] FKFS: Stuttgart Handling Roadway 3D Vehicle dynamics under laboratory conditions.  
[https://www.fkfs.de/fileadmin/FKFS/4\\_Aktuelles/Pressebilder/Flyer\\_HRW.pdf](https://www.fkfs.de/fileadmin/FKFS/4_Aktuelles/Pressebilder/Flyer_HRW.pdf), (accessed Aug. 30, 2023)
- [6] Beyerer, J., Puente León, F., Frese C.: Automatische Sichtprüfung, Heidelberg 2016, <https://doi.org/10.1007/978-3-662-47786-1>
- [7] MICRO EPSILON: Laser-Scanner für industrielle Anwendung scanCONTROL 25x0  
<https://www.micro-epsilon.de/download/products/cat-scancontrol/dax--scanCONTROL-25x0--de.html#page=2&zoom=Fit>, (accessed Aug. 28, 2023)
- [8] Blum F.: 2D/3D-Laserscanner mit roter und blauer Laserdiode von Micro-Epsilon  
<https://www.ke-next.de/automation/sensorik-messtechnik/id-2d3d-laserscanner-mit-roter-und-blauer-laserdiode-von-micro-epsilon-306.html>, (accessed Sept. 04, 2023)